Accepted Manuscript

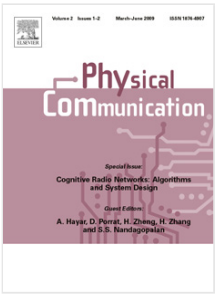

Multiple description transform coded transmission over OFDM broadcast channels

Ashwani Sharma, Swades De, Hari M. Gupta, Ranjan Gangopadhyay

PII: S1874-4907(14)00047-0
DOI: http://dx.doi.org/10.1016/j.phycom.2014.05.001
Reference: PHYCOM 255

To appear in: *Physical Communication*

Received date: 31 December 2012
Revised date: 8 May 2014
Accepted date: 9 May 2014

Please cite this article as: A. Sharma, S. De, H.M. Gupta, R. Gangopadhyay, Multiple description transform coded transmission over OFDM broadcast channels, *Physical Communication* (2014), http://dx.doi.org/10.1016/j.phycom.2014.05.001

Multiple Description Transform Coded Transmission over OFDM Broadcast Channels

Ashwani Sharma[a], Swades De[b,*], Hari M. Gupta[b], Ranjan Gangopadhyay[c]

[a]*Mobility Group, DuestoTech, University of Duesto, Bilbao, Spain*
[b]*Electrical Engineering Dept. and Bharti School of Telecom, Indian Institute of Technology Delhi, New Delhi, India*
[c]*The LNM Institute of Information Technology, Jaipur, India*

Abstract

We consider image transmission using multiple description transform coding (MDTC) over orthogonal frequency division multiplexed (OFDM) wireless broadcast channels, where the system may not have any feedback on channel gains. We investigate the redundancy allocation in MDTC-OFDM system, physical layer frequency diversity, and decoding strategies to maximize the quality of reconstruction. Via mathematical analysis, supported by MATLAB simulations, we show that, error resilience of the descriptions can be increased by suitable assignment of coding redundancy in the transform modules at the source, which can be further optimized if the channel characteristics are known at the transmitter. Additionally, the relative performance of the MDTC-OFDM system is studied with respect to a competitive approach, called forward error correction based multiple description coding (MDC) over OFDM, where we show that, for the same redundancy assignment, the MDTC based system performs better under harsh channel conditions.

Keywords: Multiple description transform coding; source coding redundancy; MDTC-OFDM system; feedback-less broadcast channel; frequency diversity; MDTC estimation

1. Introduction

There are three types of coding normally practiced for image/video content: non-progressive coding, progressive (layered) coding, and multiple description coding (MDC). In MDC, the MD

*Corresponding author. Tel.: +91.11.2659.1042; fax: +91.11.2658.1606.
Email addresses: ashwani.maharaj@gmail.com (Ashwani Sharma), swadesd@ee.iitd.ac.in (Swades De), hmgupta@ee.iitd.ac.in (Hari M. Gupta), ranjan_iitkgp@yahoo.com (Ranjan Gangopadhyay)

coder generates multiple descriptions or message blocks from the source content. The generated descriptions are such that they are correlated with each other. This correlatedness feature is introduced by adding some controlled redundancy or extra bits to the compressed source data. This process helps to estimate the lost (corrupted) descriptions from the correctly received ones and thus retransmissions can be avoided [1], but it is at the cost of a reduced compression efficiency. MDC is a more robust technique for wireless environments, as an MDC receiver can decode the data with a low but acceptable image quality even if some of the descriptions are lost [2].

At the physical transmission level, orthogonal frequency division multiplexing (OFDM) is used in many current wireless communication systems, as it provides an opportunity to exploit the diversity in frequency domain by providing a number of sub-carriers, which can work as multiple flat fading channels for applications dealing with multiple bit streams.

Combinedly, MDC at the source along with OFDM at the physical layer is an interesting alternative image/video coding technique to combat bursty packet losses over wireless channels, and it is especially promising for applications where retransmission is unacceptable.

1.1. Background and motivation

The simplest way to produce multiple descriptions is to partition the raw source content into the required number of sets and compress them independently. For description recovery, interpolation techniques are used [3]. Scalar quantization based MDC (called MDSQ) is another technique that was introduced in [4]. The recent advancements in this area are Gram-Schmidt orthogonalization based multiple description quantization (MDQ) [5] and the one via delta-sigma modulation [6]. Another recent development is lattice vector quantization based multiple descriptions (MDLVQ) generation [7, 8], that exploits the correlation among the source samples. Multiple description transform coding (MDTC) is another variant of MDC, that was introduced in [9, 10] and further extended in [11]. In MDTC, a correlating transform is used to introduce dependency among the coefficients (by adding redundancy or extra bits per coefficient), so that they can be estimated from each other, albeit with some distortion in the reconstructed data at the receiver. Besides the above techniques at the source level, forward error correction (FEC) based joint source-channel coding, called FEC-MDC [12, 13], has been another popular approach that works based on the channel

state information (CSI). Among these several variants, namely, quantization based (e.g., MDSQ, MDVQ), transformed based (i.e., MDTC), and FEC based MDC, *MDTC has the benefit of higher coding efficiency relative to MDQ techniques* [10]. *MDTC also enjoys simplicity and widespread compatibility with any source compression algorithm compared to FEC-MDC* [12, 9, 13].

The use of FEC variants for transmission of delay constrained contents, such as image/video, with or without involving MDC has been studied in different systems. For example, for video transmission over wireless [14], packet interleaving is combined with dynamic FEC to combat burst errors. Particularly, the packet interleaving and FEC was adapted with respect to packet deadlines, packet priority, and buffer occupancy, to improve the quality of delivered content. In [15], unequal error protection (UEP) for progressively encoded image transmission over *single carrier* wireless system with Rayleigh fading channels was studied where hierarchical modulation techniques were considered. The study in [16] provided a lucid description of performance and complexity issues associated with MDC and UEP-FEC schemes for image and video transmissions.

For image frame transmission, MDTC is generally applied on a compressed frame. It could be based on either discrete cosine transform (DCT) or discrete wavelet transform (DWT). In [11], a general framework based on square linear transform on MDTC to generate more than two descriptions from DCT coefficients was presented. For a two-description case (i.e., 2×2 transform), a simple optimal transform was proposed that produces a balanced rate for the two channels, where the redundancy-distortion trade-off can be controlled by a single parameter in the transform matrix. For realizing MDC with more than two descriptions, the authors also proposed a cascade structure for MDTC to maintain the ease of design. *To our best knowledge, the important aspect of optimal redundancy allocation, which helps maximize the description recovery in the face of transmission errors with the minimum possible overhead of data rate, is still missing in the literature.*

Between DCT based and DWT based MDTC variants, the latter was shown to be more robust to noise [17]. DCT-MDTC principles were applied on DWT images in [17]. The new system was called DWT-MDTC. The relative performance of DCT-MDTC and DWT-MDTC under varying number of received descriptions showed that the DWT-MDTC performs better under lossy scenarios. *Along this line, our interest is to analytically formulate the MDTC estimation and distortion*

associated with the losses by accounting the actual physical channel behavior.

As prior research has demonstrated, physical layer diversity also has an important role along with MDC for an optimum system performance [18, 19]. Several physical layer works, e.g., priority based protection scheme [20], rate-distortion performance [21], optimal rate allocation in MD coded transmission [22], studied the channel diversity issues based on the premise of independent erasure channels. FEC-based MDC over OFDM (FEC-MDC-OFDM) system performance was evaluated [23] and mathematically analyzed [24] under the block fading channels. The study was extended in frequency selective fast fading channel environment [25]. The application of FEC-MDC for scalable video transmission over OFDM channels was also carried out in [26]. The discussion on video transmission is however out of scope of this paper. In these studies cross-layer diversity gain was obtained from frequency selectivity of fading channels. For distortion performance measure in [23, 24, 25], the number of descriptions was set equal to the number of OFDM sub-channels. However, the description loss probability in such fading environments is highly dependent on the application layer diversity. In other words, *characterizing the distortion function in FEC-based MDC over OFDM channels would be more involved in a frequency selective fading environment if the number of descriptions is much less than the number of sub-channels.* Also, *the error protection overhead added to each application layer coded (layered) description in FEC-based MDC is dependent on image/video characteristics* (e.g., contrast, frame rate).

Although MDTC-OFDM system offers a simpler alternative to MD quantization variants and FEC-based MDC, the performance of MDTC with two or more descriptions over OFDM channels has not been adequately studied in the literature. These considerations along with the lack of CSI feedback in broadcast channels motivate us to investigate the MDTC performance over fading channels with OFDM-based physical layer.

1.2. Contribution

In this paper, the optimization of DWT-MDTC transmission over OFDM fading broadcast channels is investigated with an implicit assumption of a symmetric MDC (where the descriptions are equally important). The major contributions in this paper are the following:

1. To aid applicability of the proposed MDTC-OFDM scheme on any image frames, a gener-

alized parametric function, which models how the image is compressed based on the image frame's quality factor (e.g., sharpness, contrast), is introduced.

2. A channel-aware MDTC-OFDM system is designed by optimally assigning the redundancy to minimize the average distortion. It is shown that the error resilience of the descriptions can be increased by suitable assignment of coding redundancy in the transform modules at the source and by exploiting physical layer frequency diversity and channel feedback. *It may be noted that, optimum redundancy allocation in MDC descriptions for a given total redundancy is critical for minimized distortion of the application content at the receiver.*
3. A sub-optimal method, which is solely based on the quality factor of the image and the redundancy allocation at the source, is developed for channel-oblivious MDTC-OFDM system for broadcast channels. The performance of the proposed method for the channel-oblivious MDTC-OFDM system is compared with that of the channel-aware MDTC-OFDM system. In addition, an efficient MDTC decoding (estimation) technique is proposed to maximize the image reception quality.

A comparative study of the proposed MDTC-OFDM system with a competitive scheme (FEC-MDC-OFDM) shows that the MDTC-OFDM system performs better under harsh channel condition.

1.3. Organization

The rest of the paper is organized as follows. Section 2 describes the MDTC-OFDM system model, the proposed parametric model that generically represents a compressed source, the cascade structure for the MDTC along with the estimation approach, the channel model, and MDTC descriptions mapping over the OFDM channels. Section 3 contains the distortion analysis, fading channel dependent error performance, and optimization formulation on redundancy allocation. Section 4 presents the numerical optimization procedure and the results on channel feedback based optimum redundancy allocation and channel-oblivious sub-optimal redundancy allocation performance, followed by a comparative performance study of MDTC-OFDM and FEC-MDC-OFDM systems in Section 5. The paper is concluded in Section 6.

2. System model

2.1. MDTC-OFDM system

An example of the proposed MDTC-OFDM system model is depicted in Fig. 1. Following the

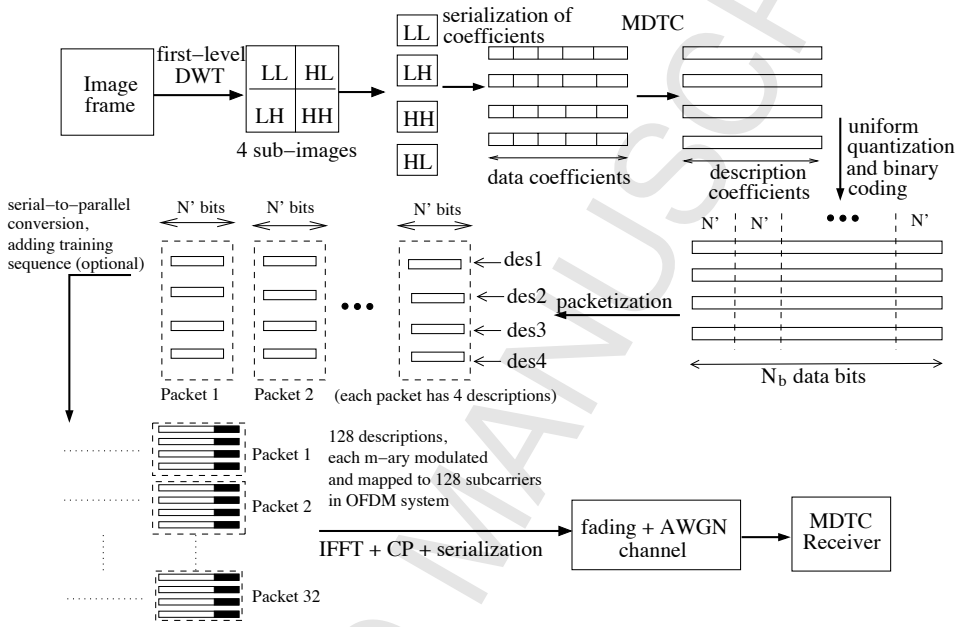

Figure 1: An example of MDTC-OFDM system with 4 descriptions and 128 sub-channels.

JPEG-2000 standard [27], an image is compressed using 2-dimensional DWT, on which MDTC is applied. The generated descriptions are suitably arranged and fed to the OFDM system with the same fixed modulation scheme for each sub-carrier[1]. Suitable estimation techniques are applied for error recovery at the receiver end, so as to minimize the distortion.

In 2-dimensional DWT, the minimum number of descriptions generated out of an image frame (after first-level compression) is 4. So, the MDTC scheme has to operate with a minimum 4 descriptions. The compression process can be extended to multi-level DWT and the proposed

[1]In general, the term *sub-carrier* refers to one of the carriers (i.e., a narrow-band frequency channel) in a multicarrier (OFDM) system, whereas a *sub-channel* can refer to a single narrow-band channel or more than one (contiguous or dispersed) such narrow-band channels. In this paper, the frequency band around a single sub-carrier is considered as a sub-channel, and so the two terminologies are synonymously used here.

MDTC-OFDM system model would work with any number of descriptions (in multiples of 2) by extending the cascading structure, although the numerical computation for optimum redundancy assignment in MDTC becomes more involved with the increased number of descriptions (Section 3). Furthermore, it was demonstrated in [28] that the increase in performance gain slows down significantly as the number of descriptions is increased beyond 2. Driven by these practical observations, we argue that the general MDTC-OFDM system is not of interest, and we choose to work with 4 descriptions MDTC system. The number of OFDM sub-carriers can be chosen as per the wireless access system physical layer standards. In our analysis (Section 3), 128 sub-carriers have been considered. The functional steps involved in MDTC-OFDM system are as follows:

1) First-level DWT is applied on an image frame producing 4 sub-images: HL, LH, HH, and LL. If the original frame is of size $N_1 \times N_2$ pixels, then each sub-image is of size $\frac{N_1}{2} \times \frac{N_2}{2}$ pixels.

2) From the 4 sub-images 4 *data coefficient vectors* are generated by fetching them serially. For a sub-image of size $\frac{N_1}{2} \times \frac{N_2}{2}$ pixels, the number of coefficients in each data coefficient vector is $\frac{N_1 N_2}{4}$.

3) Adopting the techniques in [29], MDTC cascading is applied on 4 coefficients - one each from a data coefficient vector - to get 4 correlated coefficients (detailed in Section 2.3).

4) Step 3 is repeated for all coefficients in the data vectors. Thus, 4 correlated *description coefficient vectors* are generated, each of length $\frac{N_1 N_2}{4}$.

5) The description coefficient vectors are uniformly quantized and binary coded with L bits/ coefficient, to form the *description bit vectors*, each of length $N_b = \frac{N_1 N_2 L}{4}$ bits.

6) The description bit vectors are collated and mapped onto the OFDM system (Section 2.5), and a suitable estimation technique is used for the lost (corrupted) description recovery at the receiver (Section 2.3).

2.2. Model to generate compressed source vectors

We note that, variances of the compressed data vector depend on the image as well as the compression technique used. For a comprehensive study on different sources, we introduce a generalized parametric function,

$$\psi_i = a(v)(i-1)^v + b(v), \tag{1}$$

the slope of which represents the relative difference in variances among the compressed image coefficients. By adjusting the variance controlling parameter (quality factor) v, the variances of different data vectors of any given compressed image can be realized. In (1), the coefficients $a(v)$ and $b(v)$ are functions of v. The values of ψ_i provide the corresponding relative measures of variances $\sigma^2_{x_i}$, for $1 \leq i \leq 4$. $a(v)$ and $b(v)$ are suitably chosen to control the absolute values of the variances of the compressed source. We normalize the variances with respect to the highest value $\sigma^2_{x_1}$, with $\sigma^2_{x_1} = 1$, which corresponds to $b(v) = 1$. $a(v)$ is obtained by setting $\psi_i = 0$ at $i = 5$, which gives $a(v) = -0.25^v$. This model of generating compressed source vectors gives the variances as: $\sigma^2_{x_1} = 1$; $\sigma^2_{x_2} = 1 - 0.25^v$; $\sigma^2_{x_3} = 1 - 0.5^v$; $\sigma^2_{x_4} = 1 - 0.75^v$. Fig. 2 shows the four

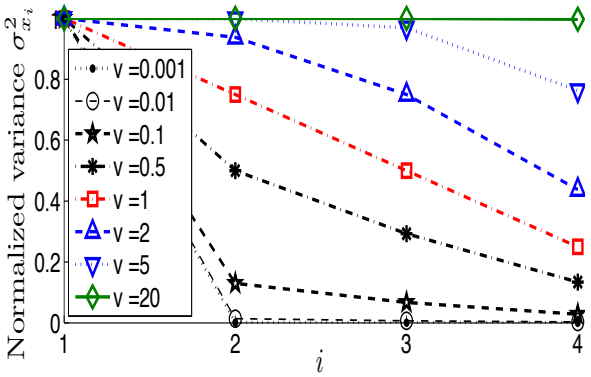

Figure 2: Considered source generating system: different source vector variances with parameter v.

source vector variances, generated with different values of v. It can be noted that, a higher value of v corresponds to a lesser difference among the variances $\sigma^2_{x_i}$. Moreover, applying MDC over the data vectors with equal or nearly equal variances does not contribute to any reduction in distortion, because the mean square distortion (MSD) of a received MDC image frame is respectively upper and lower bounded by the average and minimum variances [29]. Accordingly, in this study, we have concentrated on lower values of v. (Our results are valid for all values for v. However, higher values are not of much practical interest. We studied the variances of data over several DWT compressed test images and found that in no cases all the variances are close to each other. Standard Lena image is best matched with $v = .02$, whereas for the other image frames, the value of v lies in the range of 0.001 and 1.)

2.3. MDTC Cascading Structure and estimation

Fig. 3 shows the pair-wise correlating transform module and the cascade structure for generating 4 descriptions. X_1, X_2, X_3, and X_4 are the input data vectors; Y_1, Y_2, Y_3, and Y_4 are the output

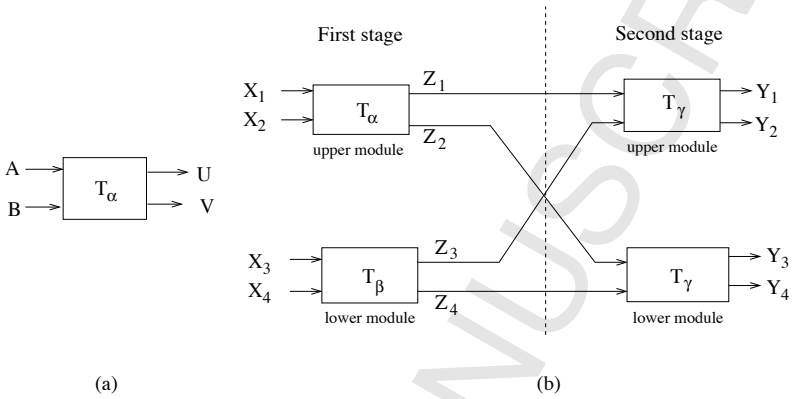

Figure 3: MDTC construction building blocks: (a) pairwise correlating transform module; (b) cascading structure to generate more than 2 descriptions.

description vectors. The amount of correlation in the output vectors depends on the redundancies put in the transform matrices T_α, T_β, and T_γ. The descriptions y_i's, which are the elements of the data vector Y_i ($i = 1, 2, 3, 4$), are transmitted over the fading channels.

At the receiver, depending on the number of descriptions received, different loss events can occur. The receiver's job is to estimate $\hat{y}_i$'s and subsequently $\hat{x}_i$'s via MDTC estimation and inverse transforms. (Note that, even if there is no loss event in the transmission process, due to quantization distortion the estimated data coefficient $\hat{x}_i$ at the receiver will be different from the original x_i at the transmitter.) The estimation technique to regenerate the lost (or corrupted) descriptions would decide the amount of distortion introduced. *There has been no standard MDTC estimation technique available in the literature for the cascading structure.* To this end, we analyze and compare two estimation techniques, denoted as ET_1 and ET_2. MDTC cascading structure (Fig. 3(b)) has two stages, each consisting of two modules. The estimation approach is described below, where the distinct cases for ET_1 and ET_2 are highlighted.

(i) If all descriptions are received, no distortion due to MDTC estimation is introduced, as no MDTC estimation is needed.

(ii) If only one description is lost, estimation is done in the corresponding module at the second stage. For example, if y_1 is lost, it is estimated at the second upper module using $\hat{y}_2$.

(iii) With two descriptions lost, two cases are possible:

Case a: If the lost descriptions belong to different correlating modules, estimation is done at both the modules of the second stage. For example, if y_1 and y_3 are lost, $\hat{y}_1$ is estimated at the second upper module using $\hat{y}_2$, and $\hat{y}_3$ is estimated at the second lower module using $\hat{y}_4$.

Case b: If the lost descriptions belong to the same correlating module, in ET_1, the input coefficients corresponding to the lost descriptions are estimated by their respective average values. For example, if y_1 and y_2 are lost, $\hat{z}_1$ and $\hat{z}_3$ are unavailable and are replaced by their respective averages. In ET_2, on the other hand, the estimation is done at the first stage. For example, if y_1 and y_2 are lost, then consider as if $\hat{z}_1$ and $\hat{z}_3$ are unavailable. Since $\hat{y}_3$ and $\hat{y}_4$ are successfully received, $\hat{z}_2$ and $\hat{z}_4$ are known by inverse transform without added distortion due to estimation. Then, $\hat{z}_1$ is estimated at the first upper module using $\hat{z}_2$, and $\hat{z}_3$ is estimated at the first lower module using $\hat{z}_4$.

(iv) Three description loss is equivalent to the occurrence of events (ii) and (iii-b) jointly. For example, consider y_1, y_2, and y_3 are lost simultaneously. In both ET_1 and ET_2, $\hat{y}_3$ is estimated at the second lower module using $\hat{y}_4$. In ET_1, estimates of $\hat{z}_1$ and $\hat{z}_3$ are their respective average values. In ET_2, $\hat{z}_1$ will be estimated using $\hat{z}_2$ in the first upper module, and $\hat{z}_3$ will be estimated using $\hat{z}_4$ in the first lower module.

(v) If all descriptions are lost, then simply all $\hat{x}_i$'s are estimated as their respective average values.

2.4. Channel model

In this study we use block fading channel model in time as well as frequency domains. Denoting the coherence bandwidth in terms of the number of sub-channels as M, in a block fading environment M consecutive sub-channels experience a channel gain with correlation ≈ 1, which means, they behave similarly; either all, or none, of them can be in deep fading state. Each set of such M consecutive sub-channels is called a 'sub-band'. If there are S such sub-bands, the total number of sub-carriers in the system is $K = S \cdot M$. All sub-bands are considered independently faded with Rayleigh distributed envelope, which corresponds to the block fading approximation in

frequency domain [30]. In time domain, with block fading assumption, channel fading coefficients remain constant throughout the transmission period of a description of length N' bits (cf. Fig. 1), and they change independently during the next description transmission interval.

In the MDTC-OFDM system with interleaved mapping of 4 descriptions of each packet to 4 different sub-channels (refer to Section 2.5), the loss probabilities are independent as long as $M < K/4$, which implies that each description in a packet will experience independent fading condition.

2.5. Collating the descriptions and mapping to OFDM system

As shown in Fig. 1, before collating we have 4 description bit vectors. Each vector of length N_b bits is chopped into N' bit descriptions. Four such N' bits from 4 description bit vectors are contained in a *packet*. (Note that, the term *packet* is meaningful only for mapping of the descriptions on to the sub-channels - contiguous or interleaved - which determines the correlatedness of description errors over fading channels.) Cyclic redundancy check is appended to each N' bits content for error detection. For transmitting through K sub-channels in a OFDM system, $K/4$ such packets are arranged in parallel, to get K bit streams. Training bits are optionally added at the front of each description for estimating CSI at the receiver [31]. Alternatively, a combination of block and comb based pilot signals can also be used for the CSI estimation. Since CSI may not be available in broadcast communications, each description is m-ary (nonadaptive) modulated, and the symbols are IFFT (inverse fast Fourier transform) one-to-one mapped to specific sub-channels such that all bits from one description go through the same sub-channel.

Since the MDTC recovery performance depends on how the correlated descriptions belonging to the same packet are mapped to sub-channels, to achieve the highest gain from the application layer diversity (by MDC), physical layer diversity must be exploited. To this effect, we consider an *interleaved sub-channel mapping* scheme to ensure that all descriptions from the same packet are transmitted through the sub-channels that can be as far apart from each other as possible so that they are less likely to be simultaneously affected by block fading. *Intuitively, in absence of channel feedback, as in broadcast communications, interleaved sub-channel mapping is the best possible channel assignment for MD coded transmission.* This physical layer diversity plays a critical role

because the number of sub-channels K is much higher than the number of descriptions that are to be mapped, and the transmitter in broadcast communications may not have the accurate CSI.

3. Distortion Analysis of MDTC-OFDM System

We now analyze and optimize the performance of the MDTC-OFDM system.

3.1. Distortion associated with 4-description MDTC system

3.1.1. Pair-wise correlation unit

In 2-description MDTC, the distortion measures are given below [29]. Referring to Fig. 3(a), T_α is the pair-wise correlating transform matrix and is given as:

$$T_\alpha = \begin{pmatrix} \alpha & \frac{1}{2\alpha} \\ -\alpha & \frac{1}{2\alpha} \end{pmatrix}. \tag{2}$$

The corresponding input-output coefficients relationship is: $\begin{pmatrix} u \\ v \end{pmatrix} = T_\alpha \begin{pmatrix} a \\ b \end{pmatrix}$. Denoting the redundancy introduced in MDTC as ρ bits/coefficient, the parameter α in (2) can be calculated from

$$\alpha = \sqrt{\frac{\sigma_b}{2\sigma_a(2^\rho - \sqrt{2^{2\rho}-1})}}, \tag{3}$$

where σ_a^2 and σ_b^2 are the variances of a and b, respectively.

The step size for the uniform quantizer is defined as Δ. If both descriptions are received correctly, the distortion is only due to quantization noise, and is given by:

$$D_{11} = \frac{\Delta^2}{6}. \tag{4}$$

The quantization distortion is much lower than that due to MDTC estimation, and hence it is ignored in estimation related cases. Thus, if both descriptions are lost, the distortion due to MDTC estimation is:

$$D_{00} = \sigma_a^2 + \sigma_b^2. \tag{5}$$

If either one of the two descriptions is lost, the distortion due to estimation of the lost description is:

$$D_{01} = D_{10} = \frac{(\alpha^2 + \frac{1}{4\alpha^2})\,\sigma_a^2\,\sigma_b^2}{\alpha^2\sigma_a^2 + \frac{1}{4\alpha^2}\sigma_b^2}. \tag{6}$$

3.1.2. Cascading structure

We extend the above formulation for the 2-stage 4×4 cascading structure (see Fig. 3(b)). T_α, T_β, and T_γ are the correlating transform matrices with the respective parameters α, β, and γ. The redundancy distributed among the four transform modules are ρ_1, ρ_2, ρ_3, and ρ_3, respectively. As in (3), α, β, and γ are calculated from:

$$\alpha = \sqrt{\frac{\sigma_{x_2}}{2\sigma_{x_1}(2^{\rho_1} - \sqrt{2^{2\rho_1} - 1})}},\ \beta = \sqrt{\frac{\sigma_{x_4}}{2\sigma_{x_3}(2^{\rho_2} - \sqrt{2^{2\rho_2} - 1})}},\ \gamma = \sqrt{\frac{\sigma_{z_3}}{2\sigma_{z_1}(2^{\rho_3} - \sqrt{2^{2\rho_3} - 1})}}. \tag{7}$$

If the total redundancy per coefficient is ρ, then $\rho_1 + \rho_2 + 2\rho_3 = \rho$. For a given ρ, the MDTC distortion performance is a function of the distribution of ρ_i's.

The outputs of the two stages, z_i's and y_i's are:

$$z_1 = \alpha x_1 + \frac{1}{2\alpha}x_2;\ z_2 = -\alpha x_1 + \frac{1}{2\alpha}x_2; z_3 = \beta x_3 + \frac{1}{2\beta}x_4;\ z_4 = -\beta x_3 + \frac{1}{2\beta}x_4$$
$$y_1 = \gamma z_1 + \frac{1}{2\gamma}z_3;\ y_2 = -\gamma z_1 + \frac{1}{2\gamma}z_3; y_3 = \gamma z_2 + \frac{1}{2\gamma}z_4;\ y_4 = -\gamma z_2 + \frac{1}{2\gamma}z_4.$$

The respective variances of the first-stage outputs z_i's are:

$$\sigma_{z_1}^2 = \alpha^2\sigma_{x_1}^2 + \frac{1}{4\alpha^2}\sigma_{x_2}^2 = \sigma_{z_2}^2; \quad \sigma_{z_3}^2 = \beta^2\sigma_{x_3}^2 + \frac{1}{4\beta^2}\sigma_{x_4}^2 = \sigma_{z_4}^2.$$

We denote the MSD by D_i when the number of descriptions received is i ($0 \le i \le 4$). D_i can be found from D_{lll}, where $l = 0$ or 1, and the position of l indicates the state of the corresponding description. D_i associated with the lost descriptions (as described in Section 2.3) are as follows.

(i) *All four descriptions are correctly received:* In this case only the distortion due to quantization will dominate for both ET_1 and ET_2. Using (4), the MSD is:

$$D_4^{(ET_1)} = D_4^{(ET_2)} \equiv D_{1111} = \frac{2\Delta^2}{6} = \frac{\Delta^2}{3}. \tag{8}$$

(ii) *Only one description, say y_1, is lost:* In this case, the estimation is done at the second upper module for both ET_1 and ET_2. Using (4) and (6), the distortion is given by:

$$D_{0111} = \frac{\left[\gamma^2 + \frac{1}{4\gamma^2}\right]\sigma_{z_1}^2\sigma_{z_3}^2}{\gamma^2\sigma_{z_1}^2 + \frac{\sigma_{z_3}^2}{4\gamma^2}} + \frac{\Delta^2}{6}.$$

Neglecting the quantization distortion and substituting for $\sigma_{z_i}^2$:

$$D_{0111} = \frac{\left[\gamma^2 + \frac{1}{4\gamma^2}\right]\left[\alpha^2\sigma_{x_1}^2 + \frac{\sigma_{x_2}^2}{4\alpha^2}\right]\left[\beta^2\sigma_{x_3}^2 + \frac{\sigma_{x_4}^2}{4\beta^2}\right]}{\alpha^2\gamma^2\sigma_{x_1}^2 + \frac{\gamma^2\sigma_{x_2}^2}{4\alpha^2} + \frac{\beta^2\sigma_{x_3}^2}{4\gamma^2} + \frac{\sigma_{x_4}^2}{16\beta^2\gamma^2}}. \tag{9}$$

As explained in Section 2.3, by symmetry,

$$D_{0111} = D_{1011} = D_{1101} = D_{1110}. \tag{10}$$

Thus,

$$D_3^{(ET_1)} = D_3^{(ET_2)} \equiv D_{0111}. \tag{11}$$

(iii) *Two descriptions are lost:*

Case a: If the lost descriptions belong to different correlating modules, e.g., y_1 and y_3, the estimation is done at the second stage for both ET_1 and ET_2. Using (10), the corresponding distortion is:

$$D_{0101} = D_{0111} + D_{1101} = 2D_{0111},$$

Also, by inspection,

$$D_{0101} = D_{1010} = D_{1001} = D_{0110}.$$

Thus, *Case a*, with D_{0111} obtained from (9), yields the distortion for two lost descriptions as:

$$D_{2(a)}^{(ET_1)} = D_{2(a)}^{(ET_2)} \equiv 2D_{0111}. \tag{12}$$

Case b: If the lost descriptions belong to the same correlating module, ET_1 and ET_2 work differently. We have, by inspection, $D_{0011} = D_{1100}$. For the distortion calculation, assume y_1 and y_2 are lost.

In ET_1, $\hat{z}_1$ and $\hat{z}_3$ are replaced by their respective averages. Using (5), the introduced distortion is:

$$D_{2(b)}^{(ET_1)} = D_{0011}^{(ET_1)} = \sigma_{z_1}^2 + \sigma_{z_3}^2 = \alpha^2\sigma_{x_1}^2 + \frac{\sigma_{x_2}^2}{4\alpha^2} + \beta^2\sigma_{x_3}^2 + \frac{\sigma_{x_4}^2}{4\beta^2} \tag{13}$$

In ET_2, the estimation will be done at the first stage upper and lower modules with the help of correct $\hat{z}_2$ and $\hat{z}_4$, respectively. The distortion can be expressed as:

$$D_{2(b)}^{(ET_2)} = D_{0011}^{(ET_2)} = D_{01|T_\alpha} + D_{01|T_\beta}.$$

Substituting the value of D_{01} in (6) with the respective transform parameters α and β, we have:

$$D_{2(b)}^{(ET_2)} = \frac{\left[\alpha^2 + \frac{1}{4\alpha^2}\right]\sigma_{x_1}^2\sigma_{x_2}^2}{\alpha^2\sigma_{x_1}^2 + \frac{\sigma_{x_2}^2}{4\alpha^2}} + \frac{(\beta^2 + \frac{1}{4\beta^2})\sigma_{x_3}^2\sigma_{x_4}^2}{\beta^2\sigma_{x_3}^2 + \frac{\sigma_{x_4}^2}{4\beta^2}}. \tag{14}$$

(iv) *Three descriptions are lost:* Say, only y_1 is received. The distortion in ET_1 can be computed as:

$$D_{1000}^{(ET_1)} = D_{1011} + D_{1100}^{(ET_1)}, \tag{15}$$

where D_{1011} is obtained by (9) and (10), and $D_{1100}^{(ET_1)}$ is obtained from (13). Also, by inspection,

$$D_{1000}^{(ET_t)} = D_{0100}^{(ET_t)} = D_{0010}^{(ET_t)} = D_{0001}^{(ET_t)}, \quad \text{for } t = 1, 2. \tag{16}$$

Hence, the distortion in ET_1 due to receiving only one description is:

$$D_1^{(ET_1)} \equiv D_{1000}^{(ET_1)}. \tag{17}$$

In ET_2, $D_{1000}^{(ET_2)} = D_{1011} + D_{1100}^{(ET_2)}$, where $D_{1100}^{(ET_1)}$ is obtained from (14). By (16),

$$D_1^{(ET_2)} \equiv D_{1000}^{(ET_2)}. \tag{18}$$

(v) *All four descriptions are lost:* In this case, for both ET_1 and ET_2 the lost descriptions are simply represented by their respective averages, and the distortion is:

$$D_0^{(ET_1)} = D_0^{(ET_2)} \equiv D_{0000} = \sum_{i=1}^{4} \sigma_{x_i}^2. \tag{19}$$

Below, we evaluate the probabilities of receiving i descriptions under different block fading conditions.

3.2. Block fading channel behavior

To obtain the MSD, we need to compute the description loss probabilities in block fading environment. $(K/4)$ packets, each with 4 descriptions, are transmitted through K sub-channels. Recall that, the number of sub-channels is $K \gg 4$ in the proposed MDTC-OFDM system. Since the 4 sub-channels chosen for each packet are spaced apart by $K/4$ sub-carriers, as long as $M \leq K/4$, each description practically faces independent fading state. The successful reception probability of i descriptions, P_i ($i \leq 4$) depends on the fading condition faced by the 4 descriptions.

Performance of the proposed scheme depends on the probability of loss events. These probabilities are determined with respect to the channel fading parameter. In a Rayleigh channel, the instantaneous SNR $\mathbf{S}$ is exponentially distributed with probability density function (pdf) given by:

$$\mathrm{f}_{\mathbf{S}}(a) = \frac{1}{\overline{S}} exp\left(-\frac{a}{\overline{S}}\right), \tag{20}$$

where $\overline{S}$ is the average received SNR. If F is the fading margin, it is related to the receiver threshold SNR S_{th} (or deep fading threshold corresponding to an acceptable error rate for a reliable communication) as:

$$F = \frac{\overline{S}}{S_{th}}. \tag{21}$$

Let p be the probability that a sub-band is in deep fade, i.e., the received SNR is below fading threshold S_{th}. Using (20) and (21), p is obtained as:

$$p = \int_0^{S_{th}} \mathrm{f}_{\mathbf{S}}(a)\, da = 1 - exp\left(-\frac{1}{F}\right). \tag{22}$$

Note that, the threshold S_{th} is an acceptable SNR threshold corresponding to an acceptable BER for a reliable communication. S_{th} can be obtained using the error rate-SNR relationship for a chosen modulation technique. Since our current focus is on the system performance due to receiver S_{th} as well as channel quality $\overline{S}$, we take fading margin F as a variable parameter which includes both the effects, as apparent from (21).

Using (22), P_i's can be obtained as follows: All descriptions are received correctly with probability $P_4 \equiv P_{1111} = (1-p)^4$. One description loss probability is $P_3 \equiv P_{0111} + P_{1011} + P_{1101} + P_{1110} = 4p(1-p)^3$. Any two descriptions, one each from the two transform modules in the second stage of the MDTC cascade structure, are lost with probability $P_{2(a)} \equiv P_{1010} + P_{1001} + P_{0110} + P_{0101} = 4p^2(1-p)^2$. Any two descriptions, both from the same transform module in the second stage, are lost with probability $P_{2(b)} \equiv P_{0011} + P_{1100} = 2p^2(1-p)^2$. Three descriptions loss probability is $P_1 \equiv P_{1000} + P_{0100} + P_{0010} + P_{0001} = 4p^3(1-p)$. All descriptions loss probability is $P_0 \equiv P_{0000} = p^4$.

The MSD $\overline{D}^{(ET_t)}$ is obtained in terms of P_i and $D_i^{(ET_t)}$, $0 \le i \le 4$; $t = 1, 2$, as:

$$\overline{D}^{(ET_t)} = \sum_{i=0}^{4} D_i^{(ET_t)} P_i, \tag{23}$$

which includes the two separate cases of two descriptions loss: *case a* and *case b*. Note that, $D_{2(b)}$ and D_3 are different in ET_1 and ET_2, which would result in different distortion measures associated with them.

3.3. Cross-layer optimization: Channel-aware MDTC-OFDM system

We now formulate a cross-layer optimization problem which provides an optimal MDTC system design for a given fading margin F and variance parameter v. We have to find the optimal redundancy assignments ρ_1, ρ_2, and ρ_3, to minimize the MSD $\overline{D}$ in (23). Here, ET_t-dependence in $\overline{D}$ is not shown for brevity and also since the optimization is generic. The optimization problem can be formulated as:

$$\text{minimize} \quad \overline{D} \equiv \min\left\{ \sum_{i=0}^{4} D_i P_i \right\}, \text{ subject to} \quad \rho_1 + \rho_2 + 2\rho_3 = \rho, \tag{24}$$

for a given total budget ρ. This optimization problem is solved by the method of Lagrange multipliers. We introduce a Lagrange multiplier λ and the Lagrange function defined by

$$\pounds(\rho_1, \rho_2, \rho_3, \lambda) = \sum_{i=0}^{4} D_i P_i + \lambda(\rho_1 + \rho_2 + 2\rho_3 - \rho).$$

The solution for optimum redundancy that minimizes $\overline{D}$ are the points where the partial derivatives of $\pounds$ with respect to ρ_1, ρ_2, ρ_3, λ are zero. It satisfy the four non-linear equations, obtained as:

$$\begin{aligned}
&\triangle(\pounds, \rho_1) = 0, \quad \text{i.e., } \triangle(\sigma_{z_1}^2, \rho_1) \cdot \left[\frac{K_0 \left(\frac{1}{4} + \frac{1}{16\gamma^4} \right) \sigma_{z_3}^4}{\left(\gamma^2 \sigma_{z_1}^2 + \frac{\sigma_{z_3}^2}{4\gamma^2} \right)^2} + K_1 \right] + \lambda = 0, \\
&\triangle(\pounds, \rho_2) = 0, \quad \text{i.e., } \triangle(\sigma_{z_3}^2, \rho_2) \cdot \left[\frac{K_0 \left(\gamma^4 + \frac{1}{4} \right) \sigma_{z_1}^4}{\left(\gamma^2 \sigma_{z_1}^2 + \frac{\sigma_{z_3}^2}{4\gamma^2} \right)^2} + K_1 \right] + \lambda = 0, \\
&\triangle(\pounds, \rho_3) = 0, \quad \text{i.e., } \triangle(\gamma^2, \rho_3) \cdot \left[\frac{K_0 \left(\sigma_{z_3}^2 - \sigma_{z_1}^2 \right) \sigma_{z_1}^2 \sigma_{z_3}^2}{2\gamma^2 \left(\gamma^2 \sigma_{z_1}^2 + \frac{\sigma_{z_3}^2}{4\gamma^2} \right)^2} \right] + 2\lambda = 0, \\
&\triangle(\pounds, \lambda) = 0, \quad \text{i.e., } \rho_1 + \rho_2 + 2\rho_3 - \rho = 0,
\end{aligned} \tag{25}$$

where $\triangle\big(Q(q), q\big)$ is the partial derivative of $Q(q)$ with respect to q. K_0 and K_1 are respectively defined as $K_0 = P_1 + P_3 + 2P_{2(a)}$ and $K_1 = P_1 + 2P_{2(b)}$. The set of equations (25) involves

complex nonlinear terms and it is difficult to obtain a closed form solution. We use numerical methods to solve this optimization problem. The results are discussed in Section 4.3.

4. Performance Studies and Results

We have performed numerical studies in MATLAB to evaluate and optimize the performance of MDTC-OFDM system (shown in Fig. 1). MDTC cascading was used to generate 4 descriptions. After cascaded transform coding and digitization, packets were formed by taking $N^{'}$ bits from each of the four N_b bit data. 4 descriptions from each packet were parallelly mapped to 4 sub-channels in a $K = 128$ sub-carrier OFDM system. In this way, 32 packets are transmitted simultaneously. QPSK modulation was used for all sub-channels. Although the proposed MDTC-OFDM system would work for any coherence bandwidth, the uncorrelated loss of descriptions in a packet, which has been assumed in our analysis, requires that coherence bandwidth $M < 32$. That is, the analysis is valid as long as the fading is frequency flat over one sub-carrier (which is assumed true for OFDM channels) and the flatness is less than 32 carriers.

Since our study in this paper is for transmission over broadcast channels, e.g., broadcast streaming from a base station to the users, where channel gains feedback is unlikely to be available, our channel mapping assumes no channel gains feedback. Therefore, channel quality dependent protection or power allocation were considered impractical. A slow fading channel was assumed with coherence time larger than a packet transmission time and $M \leq K/4$. The length $N^{'}$ was chosen accordingly, to ensure that each packet transmission time is shorter than the channel coherence time in a block fading scenario.

In our study we have taken $N^{'} = 512$ bits. The quasi-static assumption requires that the channel gain is constant over the time transmission of N' bits. For a given channel rate, say 10 Mbps and $K = 128$ sub-carriers, packet transmission time $T \approx 6$ ms. If the relative speed of the receiver with respect to the transmitter is ≈ 5 m/s (or 18 kmph), the coherence time $T_c \approx 12$ ms, which is much greater than T. If the environment is more agile, i.e., if the coherence time is lesser, the description size N' can be accordingly curtailed. Therefore, the coherence time assumption is not unreasonable for any physical layer standards.

4.1. *Effect of fading channel on reception probabilities*

First, the impact of channel fading is studied in terms of successful reception probabilities P_i, $0 \leq i \leq 4$, within a packet (derived in Section 3.2). This knowledge is used in deciding MDTC construction as well as estimation techniques. Fig. 4 shows the loss probability patterns at different values of F, from where it can be concluded that the probabilities of simultaneously losing more descriptions are comparatively lower at higher fading margins. Also, one can observe

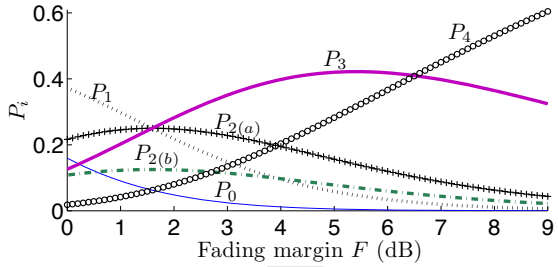

Figure 4: Description reception probability P_i at different channel fading margin F.

the convexity or monotonicity of the loss probabilities. These trends impact the effective distortion in *channel-oblivious MDTC-OFDM* system (discussed in Section 4.4).

4.2. *Estimation technique dependent distortion performance*

From the distortion analysis (Section 3) we note that, D_0 and D_4 are independent of the estimation technique. We also have in (11), $D_3^{(ET_1)} = D_3^{(ET_2)}$, and in (12), $D_{2(a)}^{(ET_1)} = D_{2(a)}^{(ET_2)}$. It can be further identified from the analysis that, $D_{2(b)}^{(ET_1)} > D_{2(b)}^{(ET_2)}$ and $D_1^{(ET_1)} > D_1^{(ET_2)}$ for optimal redundancy assignments (discussed in Section 4.3). Thus, the overall distortion in ET_1 is always greater than that in ET_2. The relative distortion performance plots of ET_1 and ET_2 as functions of channel and source parameters also corroborate the above observation, which we omit here for brevity. Accordingly, our subsequent studies are based on ET_2 decoding only.

4.3. *Channel-aware MDTC-OFDM system: optimum redundancy assignment in ET$_2$*

We now find the optimal redundancy parameters, ρ , ρ_1, ρ_2, and ρ_3, for the optimization problem discussed in Section 3.3. In Fig. 5 we plot the analytically obtained MSD versus ρ_1 and ρ_2, for a

given total budget $\rho = 2$ bits/coefficient. (Note that the highest distortion plane parallel to ρ_1 and ρ_2 axes are not of interest and hence excluded.) The minima of this curve, which is the minimum

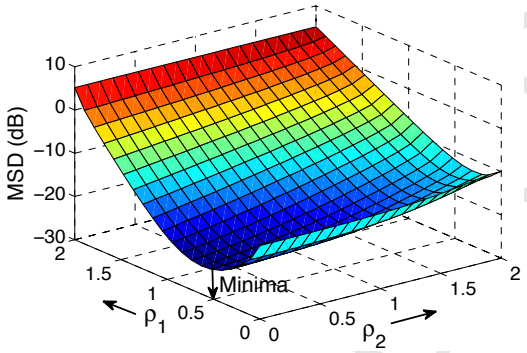

Figure 5: Average distortion versus redundancy in transform module. $\rho = 2$ bits/coefficient; $v = .001$; $F = 6$ dB.

distortion corresponding to the optimized MDTC, corresponds to the optimal values of redundancy assignment. In the numerical computation, we observed that the optimal value of ρ_2 is found to be very close zero for a given set of input parameters F, v, and ρ. This is because, the corresponding input coefficients x_3 and x_4 have much smaller variances with respect to those of x_1 and x_2 – which is the case in general for practical image frames that are characterized by $v \ll 1$. Thus, the total redundancy ρ has to be optimally distributed among ρ_1 and ρ_3 only (since the optimum $\rho_2 \approx 0$). In other words, for a given ρ, we have to find the optimum ρ_1 to achieve the minimum distortion, as ρ_3 will be adjusted automatically. As noted from Fig. 5, there should be some optimum ρ_1 to achieve a minimum MSD for a given ρ. We have used bisection method (an efficient numerical technique) to get the optimal ρ_1.

In Fig. 6(a), for a pre-assigned total redundancy ρ, the optimal ρ_1 corresponding to the minimum distortion is plotted against fading margin, where the decreasing nature of ρ_1 with F is clearly observed. This happens because, as compared to the variation of $P_2(a)$ and P_3 in Fig. 4, P_1 and $P_2(b)$ decrease with F, and ρ_1 redundancy contributes to D_1 and $D_2(b)$. From Fig. 6(a) we can also observe the relatively slow change in optimal ρ_1 for a higher value of ρ, because a higher total redundancy can sustain up to a large variation in F. The optimal ρ_1 is a function of ρ, which is also found from the figure. The maximum ρ that is allowed to be added is a trade-off between the

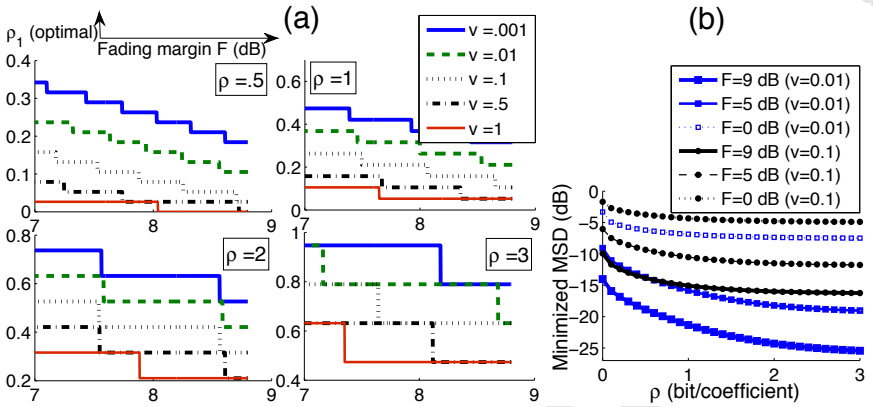

Figure 6: (a) Optimal redundancy assignment corresponding to the minimized MSD. The legends placed in the bottom-left sub-figure applies for all other plots. (b) Minimized MSD versus total redundancy budget ρ.

reception quality (benefit) and the redundancy (cost). The cost-benefit trade-off depends on the end user's choice.

In Fig. 6(b), minimized MSD versus ρ indicates that, although the quality improves with ρ, it quickly saturates. Hence, an upper limit of ρ can be decided depending on a tolerable distortion level. It can also be observed that, for a given source (e.g., $v = 0.1$) the achievable quality is greatly reduced at a lesser F and is a decreasing function of F. Thus, *if the channel does not support, the distortion can not be reduced just by increasing the redundancy budget*. Another observation is that, the quality of reception decreases with the decrease in difference among variances of source data vectors, i.e., with a higher v. This is because, MDC performs better for the sources of higher contrasts.

At this point we note that, there are only two design parameters ρ and ρ_1 for an optimal channel-aware MDTC-OFDM system. This optimization requires the channel knowledge (fading margin F, or CSI) at the application layer. Thus, if the CSI is known a-priori, an optimum ρ_1 assignment can enable to achieve a minimized mean-square distortion. However, since the CSI may not always be known, we explore to find the sub-optimal value of ρ_1 without the dynamic cross-layer message exchange, i.e., solely based on a given ρ and v at the application layer.

4.4. *Channel-oblivious MDTC-OFDM system (without cross-layer optimization)*

As suggested by the results in Section 4.3, the fading margin F (or the CSI) could help in deciding optimal redundancy distribution. But, the CSI may not be available at the transmitter in broadcast channels, and hence the distortion optimization in (24) is not possible. Yet, the source variance parameter v is known at the transmitter, which also impacts on the suitable ρ and ρ_1 assignment. Thus, although the scope of the cross-layer optimization in limited without the CSI, one can address the application layer optimization (ρ_1 assignment) which depends on the source (the parameter v) and the total redundancy allocation ρ. Here, we propose a ρ_1 assignment policy for the channel-oblivious MDTC-OFDM system.

The nature of variation of conditional distortions in Fig. 7 convey some meaningful information which can be exploited to reduce the MSD. For better interpretation of results, we divide the entire

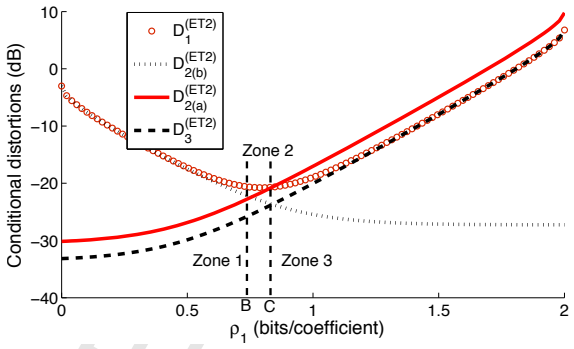

Figure 7: Variation of distortion with ρ_1. $\rho = 2$; $\rho_2 = 0$; $v = .001$.

range of ρ_1 variation into three zones. *Zone* 1 indicates the increasing trends of $D_{2(a)}^{(ET_2)}$ and $D_3^{(ET_2)}$ and decreasing trends of $D_{2(b)}^{(ET_2)}$ and $D_1^{(ET_2)}$. From Fig. 4 we observed that $P_2(a) > P_2(b)$. But, at low values of F, $P_1 > P_3$. Also, the optimal value of ρ_1 in Fig. 6(a) (the subplot with $\rho = 2$, $v = 0.001$) corresponds to point B in Fig. 7. At a higher value of F, the system incurs a lesser distortion at a lower ρ_1 but near to B, because P_3 is higher than P_1 at a higher F, causing D_3 to dominate over D_1. These observations suggest that the fixed value of ρ_1 can be taken as $\rho_{1_{(B)}}$ for improving the distortion performance at low fading margins. From the point B till C (in *zone* 2), Conditional distortions have only minor variations, and hence significant change in the

MSD is not expected when $\rho_{1_{(B)}} \leq \rho_1 \leq \rho_{1_{(C)}}$. Beyond $\rho_1 > \rho_{1_{(C)}}$ in Fig. 7, the conditional distortions are relatively higher. From Fig. 6(a) we also note that, for any values of v, ρ, and F, the channel-aware MDTC-OFDM system does never have the optimum ρ_1 values in *zone* 3. Thus, *in a channel-oblivious MDTC-OFDM system a close-to-minimum distortion performance can be achieved for a given ρ budget by restricting ρ_1 near $\rho_{1_{(B)}}$*. Hence, the point B can be set as the operating point of the system. It may be observed from Fig. 6(a) that the cross-layer optimized channel-aware MDTC-OFDM has a slowly varying ρ_1 with F, and at a lower F, the optimum $\rho_1 \approx \rho_{1_{(B)}}$. As the channel-oblivious MDTC-OFDM system is not optimized with respect to the physical layer parameters, the performance of this system is expected to be inferior to the channel-aware MDTC-OFDM system at higher values of F.

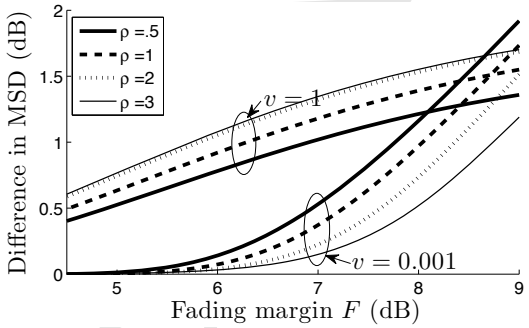

Figure 8: Loss of reception quality in channel-oblivious MDTC-OFDM with respect to channel-aware optimal MDTC-OFDM system at different fading margins.

Fig. 8 shows the performance loss of a channel-oblivious MDTC-OFDM system over the channel-aware MDTC-OFDM in terms of reception quality. It is observed that, at a typical value of the fading margin $F = 8$ dB, for an image with $v = 0.001$ and an assigned redundancy $\rho = 2$, the performance penalty with channel-oblivious MDTC-OFDM system with respect to the (channel-aware) optimal redundancy allocation is about 1.1 dB. This difference in the performance gain increases as F is increased, because the effect of P_3 dominates over that of P_1 (see Fig. 4), making the optimal value of ρ_1 further away from $\rho_{1_{(B)}}$ (see Fig. 7).

Thus, it can be noted that, in the proposed MDTC-OFDM system, although the benefit of channel oblivious redundancy allocation reduces with the increase in fading margin, quite close

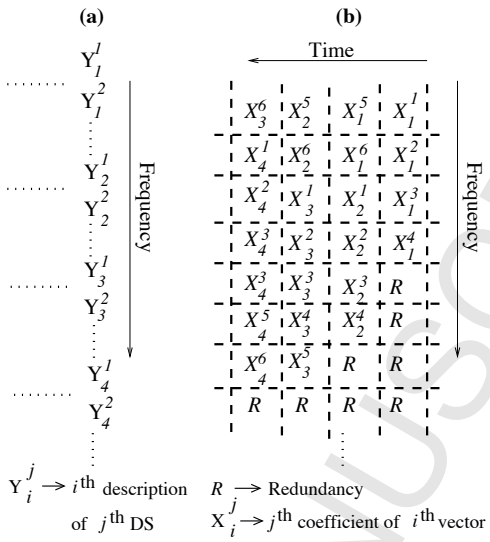

Figure 9: Comparison of the mapping schemes: (a) MDTC-OFDM; (b) FEC-MDC-OFDM (UEP scheme).

to the optimal performance can be achieved even without the knowledge of channel fading state under harsh channel conditions.

5. Comparison of MDTC with FEC-MDC

In this Section we study the MDTC-OFDM system performance relative to a recently proposed competitive approach, called FEC-MDC-OFDM [23]. We compare MDTC-OFDM system with the optimal equal error protection (EEP) as well as UEP mapping schemes of FEC-MDC-OFDM. Fig. 9 illustrates the two mapping schemes for the data coefficients (i.e., X_i and Y_i in Fig. 3), where Fig. 9(a) shows the mapping scheme described in Section 2.5 for the MDTC-OFDM system. The analytical measure of distortion associated with the MDTC-OFDM system has been quantified in Section 3. Here, we describe the analytical mean-square distortion expression for FEC-MDC-OFDM, where the optimal redundancy assignment is obtained as in [23]. An example of mapping with UEP is shown in Fig. 9(b). For the EEP scheme, the redundancy is distributed equally among all the columns. Let us assume that a column ι has R_ι bits of redundancy. Thus, for K total sub-channels, column ι would have $K - R_\iota$ number of information bits. Let the total variance of the information coefficients in column ι be σ_ι^2, which is nothing but the distortion if this column is lost.

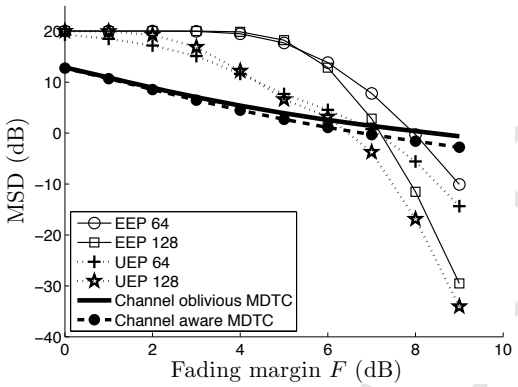

Figure 10: Comparison of MDTC-OFDM with FEC-MDC-OFDM. $\rho = 2.6$ bits/coefficient; $v = 0.02$ (corresponding to the Lena image transmission experiment).

Then, the mean-square distortion for optimal redundancy R_ι assignment is subject to minimization of the following distortion expression:

$$\overline{D}_{FEC} = \sum_{\kappa=0}^{K} \Pr[\kappa \text{ sub-channels are bad}] \times \sum_{\iota=1}^{\iota_{max}} \Psi_\iota \sigma_\iota^2, \tag{26}$$

where Ψ_ι, $\forall\ \iota$, are the conditional multipliers satisfying the condition

$$\Psi_\iota = \begin{cases} 1 & \text{if } R_\iota \leq \kappa \\ 0 & \text{otherwise} \end{cases},$$

and ι_{max} is the number of columns (i.e., the number of OFDM symbols needed to transmit the full image) in mapping. For $M = 1$, the probability expression in (26) can be written as,

$$\Pr[\kappa \text{ sub-channels are bad}] = \binom{K}{\kappa} p^\kappa (1-p)^{K-\kappa}. \tag{27}$$

The minimization of $\overline{D}_{FEC}$ in (26) provides the optimal redundancy R_ι allocation and also the minimized distortion with the UEP scheme for a given overall redundancy ρ .

Fig. 10 shows the analytical plots at different fading margin F, where two different number of sub-carriers, 64 and 128, are considered. Total redundancy for both the schemes was kept at $\rho = 2.6$ bits/coefficient. Since the bit overhead is same in the two schemes, we compare MDTC-OFDM and FEC-MDC-OFDM in terms of reception quality and computational complexity. From Fig.

10 we can observe that the MDTC-OFDM has a better performance than the FEC-MDC-OFDM schemes at lower fading margins. Thus, *the MDTC provides a higher robustness compared to the FEC-MDC in bad channel conditions (i.e., at lower values of F).* This is because, as indicated by (26) and (27), if the number of bad sub-channels κ exceeds the maximum redundancy $\max\{R_\iota\}$ (which corresponds to the most important stream), then the receiver will not be able to decode any information, leading to the complete communication outage. The chance of this outage is higher at a lower F. On the contrary, in MDTC system, redundancy is distributed at the coefficient level in such a way that even a single stream reception provides some information.

We also observe the dependency of FEC-MDC-OFDM system's performance on the number of OFDM sub-carriers. With a lower number of sub-carriers, the performance of FEC-MDC-OFDM deteriorates, whereas the performance of the MDTC-OFDM is independent of the system specification in terms of the number of sub-carriers used. The plots also demonstrate that, while the channel-oblivious MDTC-OFDM system performs poorly with respect to the channel-aware MDTC-OFDM system at a higher fading margins, it performs rather nearly equally at lower fading margins, which is also better than that of the FEC-MDC-OFDM system with EEP as well as UEP.

It is important to note that, the complexity involved in obtaining the optimal redundancy assignment in FEC-based MDC (with UEP) is very high, which increases with the number of sub-carriers in the underlying OFDM system. Specifically, the FEC-based MDC requires online computation, with the simplest algorithm for optimal FEC allocation having computational complexity $O\left(K \cdot L\right)$, where K is the number of sub-carriers in the OFDM system and L is the number of code symbols [20, 32, 23]. This is due to the iterative process of finding an optimum R_ι. In contrast, the MDTC-OFDM scheme is independent of the number of sub-carriers. In channel-aware MDTC-OFDM system one needs to perform only the ρ_1 assignment, which is a convex optimization problem and can be solved by numerical methods. For a given fading margin and a total redundancy ρ, the channel-aware MDTC-OFDM system requires $O\left(\frac{\rho}{\delta}\right)$ computations, where δ is the step size in ρ_1 assignment variation, which is much smaller compared to that in the FEC-based MDC. For example, our optimum ρ_1 studies are based on 20 steps of ρ_1 assignment. In the channel-oblivious MDTC-OFDM, the online computational complexity is further reduced to $O\left(1\right)$, as the

optimal ρ_1 assignment can be obtained by an off-line computation for a given total redundancy ρ.

6. Conclusion

In this paper we have investigated the performance of MDTC transmission of delay-constrained image/video streaming contents over OFDM broadcast channels, where there are no feedback on channel gains or having such a feedback is infeasible. At the MDTC construction stage, we have investigated optimal redundancy assignment in the transform modules and demonstrated the improvement in distortion performance at the receiver. At the recovery stage of lost descriptions, we have demonstrated that, from the knowledge of the distortion introduced by one or more description losses and applying the recovery process at the appropriate transform modules, the distortion performance can be further improved. We have studied the optimal solution for the *channel-aware MDTC-OFDM* system and discussed how closely a sub-optimal *channel-oblivious MDTC-OFDM* system can be designed. Finally, we have compared the performance of the proposed MDTC-OFDM system with that of the FEC-MDC-OFDM system and have demonstrated robustness of the proposed scheme in severe channel conditions.

Acknowledgment

This work has been supported by the Department of Science and Technology (DST) under the grant no. SR/S3/EECE/0122/2010. The authors are thankful to the anonymous reviewers for the insightful comments and valuable suggestions, which have significantly improved the quality of presentation.

References

[1] V. K. Goyal, Multiple description coding: Compression meets the network, IEEE Sig. Proc. Mag. 18 (5) (2001) 74–93.

[2] Y. C. Lee, J. Kim, Y. Altunbasak, R. M. Mersereau, Layered coded vs. multiple description coded video over error-prone networks, Signal Processing: Image Communication 18 (2003) 337–356.

[3] Y. Wang, Q.-F. Zhu, Error control and concealment for video communication: a review, Proceedings of the IEEE 86 (5) (1998) 974–997.

[4] V. Vaishampayan, Design of multiple description scalar quantizers, IEEE Trans. inform. Theory 39 (3) (1993) 821–834.

[5] Y. Frank-Dayan, R. Zamir, Dithered lattice-based quantizers for multiple descriptions, IEEE Trans. Inform. Theory 48 (1) (2002) 192–204.

[6] J. Ostergaard, R. Zamir, Multiple-description coding by dithered deltasigma quantization, IEEE Trans. Inform. Theory 55 (10) (2009) 4661–4675.

[7] V. A. Vaishampayan, N. J. A. Sloane, S. D. Servetto, Multiple-description vector quantization with lattice codebooks: design and analysis, IEEE Trans. Inform. Theory 47 (5) (2001) 1718–1734.

[8] V. K. Goyal, J. A. Kelner, J. Kovacevic, Multiple description vector quantizationwith a coarse lattice, IEEE Trans. Inform. Theory 48 (2002) 781–788.

[9] Y. Wang, M. T. Orchard, A. R. Reibman, Multiple description image coding for noisy channels by pairing transform coefficients, in: Proc. IEEE Workshop on Multimedia Sig. Proc., Princeton, NJ, 1997, pp. 419–424.

[10] M. T. Orchard, Y. Wang, V. Vaishampayan, A. R. Reibman, Redundancy rate-distortion analysis of multiple description coding using pairwise correlating transforms, in: Proc. IEEE Int. Conf. Image Proc., Santa Barbara, CA, 1997.

[11] V. K. Goyal, J. Kovacevic, Generalized multiple description coding with correlating transforms, IEEE Trans. Image Proc. 47 (2) (2001) 2199–2224.

[12] A. Albanese, J. Blomer, J. Edmonds, M. Luby, M. Sudan, Priority encoding transmission, IEEE Trans. inform. Theory 46 (6) (1996) 1737–1744.

[13] R. Puri, K. W. Lee, K. Ramchandran, V. Bharghavan, An integrated source transcoding and congestion control paradigm for video streaming in the Internet, IEEE Trans. Multimedia 3 (1) (2001) 18–32.

[14] R. Razavi, M. Fleury, M. Ghanbari, Adaptive packet-level interleaved FEC for wireless priority-encoded video streaming, Hindawi J. Advances in Multimedia 2009.

[15] S. S. Arslan, P. C. Cosman, L. B. Milstein, Coded hierarchical modulation for wireless progressive image transmission, IEEE Trans. Vehicular Technol. 60 (9) (2011) 4299–4313.

[16] E. Baccaglini, T. Tillo, G. Olmo, Image and video transmission: a comparison study of using unequal loss protection and multiple description coding, Springer Multimedia Tools and Applications: Spl. Issue Mobile Media Delivery 55 (2) (2011) 247–259.

[17] K. Khelil, R. E. H. Bekka, A. Djebari, J. M. Rouvaen, Multiple description wavelet-based image coding using correlating transforms, Int. J. Electron. Commun. 61 (2007) 411–417.

[18] J. N. Laneman, E. Martinian, G. W. Wornell, J. G. Apostolopoulos, S. J. Wee, Comparing application and physical layer approches to diversity on wireless channels, in: Proc. IEEE ICC, Anchorage, AK, USA, 2003.

[19] H. Zheng, C. Ru, L. Yu, C. W. Chen, Robust video transmission over MIMO-OFDM system using MDC and space time codes, in: Proc. IEEE Intl. Conf. Multimedia and Expo, Toronto, Ontario, Canada, 2006, pp. 633–636.

[20] A. E. Mohr, E. A. Riskin, R. E. Ladner, Graceful degradation over packet erasure channels through forward error correction, in: Proc. IEEE Data Compression Conf., 1999, pp. 92–101.

[21] S. S. Pradhan, R. Puri, K. Ramchandran, n-channel symmetric multiple descriptions - Part I: ($n,\ k$) source-channel erasure codes, IEEE Trans. inform. Theory 50 (1) (2004) 47–61.

[22] S. Zhao, D. Tuninetti, R. Ansari, D. Schonfeld, Multiple description coding over correlated multipath erasure channels, in: Proc. ICASSP, Las Vegas, NV, USA, 2008.

[23] Y. S. Chan, P. C. Cosman, L. B. Milstein, A cross-layer diversity technique for multi-carrier OFDM multimedia networks, IEEE Trans. Image Proc. 15 (4) (2006) 833–847.

[24] S.-H. Chang, P. C. Cosman, L. B. Milstein, Performance analysis of n-channel symmetric FEC-based multiple description coding for OFDM networks, IEEE Trans. Image Proc. 20 (4) (2011) 1061–1076.

[25] L. Toni, Y. S. Chan, P. C. Cosman, L. B. Milstein, Channel coding for progressive images in a 2-D time-frequency OFDM block with channel estimation errors, IEEE Trans. Image Proc. 18 (11) (2009) 2476–90.

[26] Y. S. Chan, P. C. Cosman, L. B. Milstein, A multiple description coding and delivery scheme for motion-compensated fine granularity scalable video, IEEE Trans. Image Proc. 17 (8) (2008) 1353–1367.

[27] C. Christopoulos, A. Skodras, T. Ebrahimi, The JPEG2000 still image coding system: An overview, IEEE Trans. Consumer Electron. 46 (4) (2000) 1103–1127.

[28] E. Setton, Y. Liang, B. Girod, Adaptive multiple description video streaming over multiple channels with active probing, in: Proc. Intl. Conf. Multimedia and Expo, Baltimore, MD, USA, 2003.

[29] V. K. Goyal, J. Kovacevic, Optimal multiple description transform coding of Gaussian vectors, in: Proc. IEEE Data Compression Conf., Vol. I, Snowbird, UT, 1998, pp. 388–397.

[30] M. Medard, R. G. Gallager, Bandwidth scaling for fading multipath channels, IEEE Trans. inform. Theory 48 (4) (2002) 840–852.

[31] S. Coleri, M. Ergen, A. Puri, A. Bahai, Channel estimation techniques based on pilot arrangement in OFDM system, IEEE Trans. Broadcasting 48 (3) (2002) 223–229.

[32] V. M. Stankovic, R. Hamzaoui, Z. Xiong, Real-time error protection of embedded codes for packet erasure and fading channels, IEEE Trans. Circuits, Syst., Video Technol. 14 (3) (2004) 1064–1072.

***Brief Biography**

Click here to download Brief Biography: authors_bio.txt

Ashwani Sharma received his BTech in Communication and Computer Engineering from the LN MIttal Institute of Information Technology, Jaipur, India, in 2010. During 2010-11 he worked as a Research Assistant in the Electrical Engineenring Department at IIT Delhi. He joined DeustoTech Mobility research team in Deusto Institute of Technology in 2011, and currently working towards his Ph.D in the field of Microwaves Engineering. His research interests include microwave antenna, wireless communication, and video coding.

Swades De received his Ph.D. in Electrical Eng. from the State University of New York at Buffalo, in 2004. He is currently an Associate Professor in the Department of Electrical Eng. at IIT Delhi, where he leads the Communication Networks Research Group. Before moving to IIT Delhi in 2007, he was an Assistant Professor of Electrical and Computer Eng. at NJIT (2004-–2007). He also worked as a post-doctoral researcher at ISTI-CNR, Pisa, Italy (2004), and has nearly 5 years industry experience in India in telecom hardware and software development (1993-–1997, 1999). His research interests include performance study, resource efficiency in multihop wireless and high-speed networks, broadband wireless access, and communication and systems issues in optical networks. Dr. De currently serves as an Associate Editor of IEEE Communications Letters and Springer Photonic Network Communications journal.

Hari Mohan Gupta received B.E. (Electronics and Communications) from University of Roorkee (now IIT, Roorkee) , M. Tech (UHF and Microwave Engineering) from Indian Institute of Technology, Kharagpur and Ph.D. (Electrical Engineering) from Indian Institute of Technology, Kanpur.
He joined the faculty of Electrical Engineering at Indian Institute of Technology, Delhi in 1973,where he is a professor since 1986. Prof. Gupta held positions of Head of the Department, Dean Undergraduate Studies), and Coordinator, Bharti School of elecommunication Technology and Management at IIT, Delhi. He held faculty positions at Mc Gill University, Montreal, Canada, and at Drexel University, Philadelphia, USA. He has been an academic visitor to University of Maryland, College Park, USA; Media Lab at Massachusetts Institute of Technology, Cambridge, USA; Swiss Federal Institute of Technology, Lausanne, Switzerland and several British Universities. He has been Vice-President of System Society of India, and is a founding member of Association for Security of Information Systems (ASIS). He is also President of Institution of Communication Engineers and Information Technologists (ICEIT). His research interests include mobile computing, satellite communications, multimedia information processing and photonic systems.

Ranjan Gangopadhyay did his MTech in Radiophysics and Electronics from the Univ. Calcutta and PhD from IIT Kharagpur, India. During 1980 to 2010 Prof. Gangopadhyay was with the Department of Electronics and Electrical Communication Engineering at IIT Kharagpur. Upon his rerirement from IIT Kharagpur, he has been associated with the LN Mittal Institute of Information Technology as a Distinguished Professor. Prof. Gangopadhyay has made significant contributions in the domain of Optical and Wireless Communication. His pioneering work on convolutionally coded M-ary PPM tems has a reference value providing high prospects for applications in deep-space channel and current infrared indoor communication. He has introduced a new concept of line-coding plan to counteract non-uniform FM response of DFB laser and thereby improving the performance of coherent lightwave tems. He has made a fundamental contribution to nonlinear bit synchronization and clock recovery schemes in optical receivers. He has developed a highly efficient WDM simulator for the design of high capacity optical transmission tems influenced by fiber-induced nonlinear impairment. He has contributed significantly in a number of projects in the areas of Fibre optic communication and Mobile communication, which are sponsored by national agencies such as ISRO, DRDO, MHRD, DST etc. as well as international agency like European Commission. His European Commission sponsored project on “Design of advanced wavelength-routed optical network” contributed significantly on photonic network architecture, protocols, network modeling, teletraffic analysis, design and software implementation. He was responsible in the design and development of a highly efficient simulator for WDM tem influenced by fibre-induced nonlinear impairment (1996-2000). He has accomplished an

innovative scheme for joint dispersion and nonlinearity management using optical phase conjugation and distributed Raman amplifier (2002). He put up his ardent and untiring effort in promoting, propelling and coordinating teaching and research programs in Optical Communication at the Indian Institute of Technology, Kharagpur leading to his responsible role as the coordinator of "Photonics" mission project (2002-2004). He has single-handedly established a modern Design and Simulation laboratory fully equipped with advanced software tools and Fibre optics system laboratory for conducting postgraduate teaching and research in optical and wireless communication systems. He has played a vital role in establishing international cooperation programmes with UK, Italy, Germany and Japan which turn out to be very effective in carrying out high- research programmes complementing each other's strength and expertise. His current research interests are in broadband wireless access and cognitive radio networks.

*Author Photo
Click here to download high resolution image

*Author Photo

Click here to download high resolution image

***Author Photo**
Click here to download high resolution image

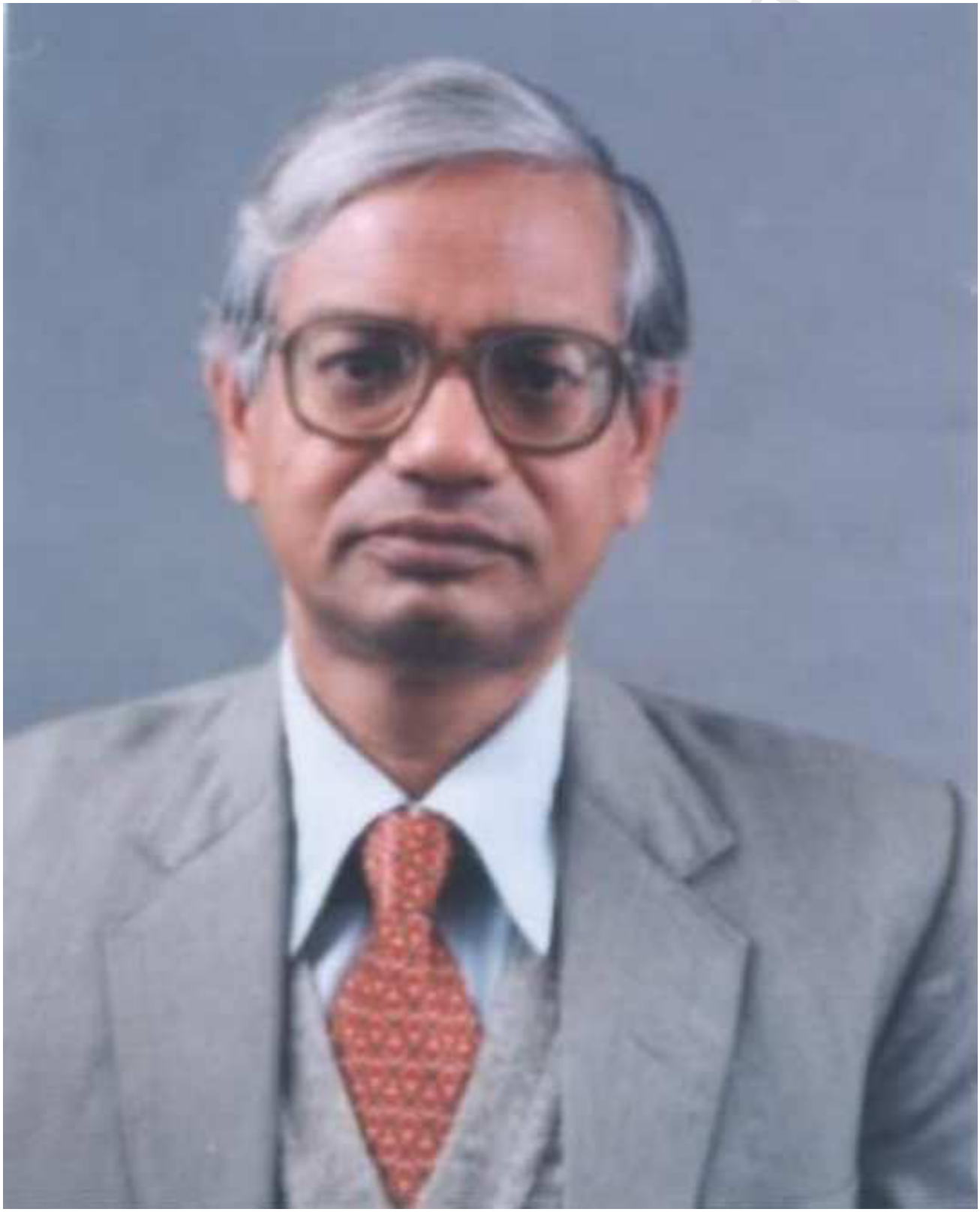

***Author Photo**
Click here to download high resolution image